Three-dimensional structures behind Glauert-Goldschmied profile under control of plasma actuation

P Prochazka[1] **and V Uruba**[1]

[1] Institute of Thermomechanics, Czech Academy of Sciences, Dolejškova 5, Praha 182 00, Czech Republic

E-mail: prochap@it.cas.cz

Abstract. The effect of plasma dielectric barrier discharge (DBD) to developed boundary layer was investigated previously. It has been shown that plasma actuation can stabilize the flow near to the surface. In the case of streamlined profile, the plasma actuation is able to shift the point of separation and hence to suppress the extent of separation area. This should lead to decrease of the form drag and increasing the total efficiency. An experimental approach is suggested for investigation and time-resolved Particle Image Velocimetry (PIV) is considered as a main measurement technique.

1. Introduction

The plasma actuation belongs to the group of active flow control strategies. These devices are relatively new in this field since their fully integration among research group is not older than one or two decades. These devices are supplied by electric current, no matter whether DC or AC. Nevertheless, the actuators, which are powered by AC current, enable to operate in unstable regime given by modulation of power signal. The laminar-to-turbulent transition (e.g. [1]) can be affected by DBD actuators as well as the shift of the separation point (e.g. [2]) and other flow field features.

The presented DBD (dielectric barrier discharge) actuator has slightly different geometry to be able to produce sufficiently strong plasma-induced flow (ionic wind) on the surface of the profile. This ionic wind affects close to the actuator surface (up to 1 mm) and is able to stabilize or destabilize the boundary layer as it was described in [3]. The actuator can be placed in spanwise orientation to produce parallel ionic with respect to the channel flow as well as in streamwise orientation to produce ionic wind perpendicularly. Normally, the actuator works in steady regime and continuous wall-jet-like flow is generated with maximal mean velocities up to 2 $m \cdot s^{-1}$. After that the rectangular modulation of the high-voltage high-frequency waveform is applied, one can observe the production of pseudo-periodical vortices inside the ionic wind - this is called as unsteady regime. This regime is very convenient due to lower power consumption demand and it allows to reach more sophisticated flow control. The vortical structures exhibit different properties given by modulation parameters and are to be used to affect the changing flow of distinct regimes around the streamlined body.

Since the study on the properties of generated vortical structures by DBD plasma actuator in steady air was performed previously [4], now this knowledge can be utilized to affect the channel flow behind an obstacle. In this study, mainly the vortex diameter, vortex trajectory, distance between two consecutive vortices, the circulation of the vortex and convective velocity of the vortex were parametrically described according to changing modulation parameters as modulation frequency and duty cycle. There is an example in equation:

$$u_{conv} = a_1 + a_2 \cdot DC + a_3 \cdot f + a_4 \cdot DC^2 + a_5 \cdot DC \cdot f + a_6 \cdot f^2 \quad (1)$$

which expresses the vortex convective velocity in dependency on modulation frequency f and duty cycle value (DC). The coefficients a_i were obtained by detailed experimental investigation.

The Glauert-Goldschmied (GG) type profile was chosen as a test profile because is commonly used for testing of the active flow control capability in numerical simulation as well as in experimental research. Some results presented in the literature will be helpful for comparison with other authors. The approach of this study is only experimental due to complexity of studied phenomenon. The results will be treated from statistical point of view when mean flow field and statistical indicator will be investigated, although the dynamics will be treated also. Since the phenomenon of vortex production is pseudo-periodical, the phase-locked measurement should be applied to highlight the dominant component of the flow.

2. Experimental layout

2.1 Actuator geometry

Every DBD actuator should consist at least of two electrodes and a dielectric layer. The wire type of DBD actuator, used during the study of boundary layer affecting along flat plate [5], has proved the ability to supplied ionic wind with sufficient velocities to influence the boundary layer and moreover its discharge and generated thrust were homogenous.

This actuator had to be rebuilt to allow the assembly on the curved profile. The dielectric layer consists of several layers of kapton foils which can be curved along the profile body. The upper electrode is made from thin tungsten wire (30μm) and is powered by HV. A series of several anchor points is utilized to lead the wire electrode across the actuator body in the specific location. Spiral torsion spring is used to make the wire uptight for all time. The lower electrode is thin layer of copper foil and it is grounded. The horizontal gap between electrodes is set to two millimeters. The actuator creates the surface of the hump profile and does not affect the flow at all.

2.2 Power source

The power source was designed and fabricated in the Institute of Thermomechanics. It is designed as a constant voltage power supply and is conceived as a half-bridge circuit excitating output high voltage ferrite transformer. The voltage value can be set linearly and the maximum peak value is 12 kV. The frequency can be also adjustable (from 10 to 30 kHz) but the constant value of 16 kHz is used as an optimum. The source has so called shutdown function which allows to use the rectangular modulation of high-voltage high-frequency waveform. The modulation brings another two parameters – modulation frequency and duty cycle – which can be used for control of the ionic wind. The velocity magnitude of the ionic wind is linearly dependent on applied voltage.

The actuator working without modulation in steady regime generates continuous wall-jet-like flow. After that the modulation is applied, the unsteady regime is set and actuator can generated a series of vortical structures called as a vortex street. The used modulation frequency determines the diameter of vortices and distance between two consecutive vortical cores. On the other hand, duty cycle determines the rate between working cycle (plasma on) of the actuator and relaxation time (plasma off) during one period. The duty cycle of 30% means that the plasma discharge is switched on for 70% of one period. Duty cycle determines the time during which the vortex is supplied by energy.

2.3 Experimental layout

The experiment was carried out in the test section connected to the blow down wind tunnel. The test section is a narrow rectangular channel with cross section dimensions of 100 x 250 mm and the length of 3000 mm. The walls of the channel had smooth surface with rectangular corners. The channel was constructed from the plexiglass plates to ensure the optical access for the laser and the cameras. The turbulence intensity level is approximately 0.1% behind the contraction. The channel velocities were varied from 5 $m \cdot s^{-1}$ to 20 $m \cdot s^{-1}$ resulting in fully developed turbulent boundary layer in desiderative location of the profile installation. The Reynolds number referred to conventional boundary layer thickness of that location can be seen from the table 1.

The Hump profile was flush-mounted to the bottom wall (the profile width was 100 mm) so that the distance from the leading edge to the contraction was 1800 mm. Two identical profiles differing in only dimensions were tested. The high of the first profile was 50 mm (20% of cross section high) and

second one was 25 mm high and 194 mm long (lower level of congestion). Further, only smaller profile will be described.

The naturally developed separation point and the size of the recirculation zone (separation bubble) were evaluated previously. The table 2. shows these results experimental acquired for the smaller hump profile. Many authors have found out that the actuator should be place as close as possible to the point of separation to have the most effective flow control. There is the question what is the exact right point of activity. Four DBD actuator location was tested for spanwise orientation when the ionic wind was generated parallel and in the same direction as the channel flow. The furthest location upstream of the separation was x/L = 0.63. The determining point of the actuator location is the wire powered electrode. This corresponds to the wire electrode location 122 mm downstream from the leading edge in horizontal sense. Next three location are x/L = 0.66, x/L = 0.69 and x/l = 0.72. The first variant has wire electrode upstream the separation, the second one is suggested to have electrode in the point of separation and the last two variants are considered downstream the separation.

The base case is referred as the flow over profile without plasma actuation. To control the size and structure of the separation bubble, the steady and mainly unsteady regimes are investigated. The plasma actuation is conducted under maximal but constant voltage value (8kV for steady and 11 kV for unsteady). The modulation frequency varies from 10 to 50 Hz during modulation. The duty cycle is set to 30 or 70%.

2.4 Measurement technique and data acquisition

To capture wake structure behind the profile, standard time-resolved PIV measurement in longitudinal plane perpendicular to the bottom side was considered. The CCD camera Phantom V711 was used to acquire the images of the flow around the profile in three distinct positions seen from the side. This camera has a resolution of 1280 x 800 pixels and corresponding maximal acquisition frequency is 6 kHz. The camera memory is 8 GB. To illuminate the tracing particles, laser New Wave Pegasus Nd:YLF is utilized. It disposes with double-head and cylindrical optics and emitted coherent light has wavelength of 527 nm. Maximal frequency is 10 kHz and pulse energy is 10 mJ for 1 kHz (10 W per head). The tracing particles were generated from safex device (droplets oil particles with diameter of 1 μm), medium image density was used.

Stereo PIV measurement in cross-section plane was suggested as a complementary measurement. Two CMOS cameras NanoSense MKIII, maximal resolution 1280 x 1024 and corresponding maximal frequency 512 double-images per second, were used. However, the acquisition time is limited due to camera memory of 4 GB. Camera chip, objectives and measurement plane did fulfill the Scheinpflug criterion. The traverse system was used to move the laser with cameras at a constant distance to measure four planes. The planes were situated at x/L = 0.69, 0.87, 1.00 and 1.50 from the leading edge.

The data acquisition was handled from three distinct points of view. The base one is to study statistical characteristic of the flow (mean flow field velocity distribution, standard deviation, etc.). That is why the lower frequency and longer measurement time was suggested (approx. 100 Hz and at least 10 seconds). To capture all fast dynamical phenomenon of boundary layer - ionic wind merging, it is necessary to use higher frequency (2 kHz) but these results will be presented only marginally. Since the production of coherent structures is pseudo-periodical phenomenon, phase-locked measurement is suggested. Then the periodic effect can be seen clearly because all random effects are averaged. Twenty phases per one period, which is given by the modulation frequency, is suggested and averaging over at least 80 periods is considered.

Table 1. The Reynolds number based on horizontal distance inlet-leading edge and on conventional BL thickness.

	Re_x	Re_δ
V_{ext} = 5 m·s^{-1}	$6 \cdot 10^5$	$10 \cdot 10^3$
V_{ext} = 10 m·s^{-1}	$12 \cdot 10^5$	$18 \cdot 10^3$
V_{ext} = 20 m·s^{-1}	$24 \cdot 10^5$	$32 \cdot 10^3$

Table 2. The separation point location and the reattachement point location for different channel velocities, examined on the Hump profile with the actuator.

V_{ext} = 5 m·s^{-1}	x/L = 0.65	x/L = 1.31
V_{ext} = 10 m·s^{-1}	x/L = 0.65	x/L = 1.12
V_{ext} = 20 m·s^{-1}	x/L = 0.65	x/L = 0.97

3. Results

Two different Hump profile sizes were tested in the channel due to congestion. The velocity increment far above the boundary layer over the hump region can be seen at the figure 1. Each color represents a different camera position. This diagram shows that the increase of the u-component is up to 14% and gradually decreases to normal value in x/L = 1.5. This test was also performed for bigger profile (25% of channel height) where the level of congestion was higher and inconvenient for DBD actuator testing. Next paragraphs will be devoted only to the smaller profile.

The figure 2 shows the velocity vector map of the ionic wind produced by the actuator in steady regime without the influence of the channel flow. The wire electrode is situated at x/L = 0.63. The maximal mean velocity is around 1 m·s^{-1} but peak value is at least two times larger. The topology of the ionic wind at little bit differs from the ionic wind over flat plate. The flow is fully attached to the curved surface due to Coanda effect. The position of maximal velocity area is very close to the surface (1-2 mm) and approximately 5 mm downstream the wire. This implies that the wire electrode position is not so important in relation to the separation point. That is why two positions upstream the separation were chosen to test.

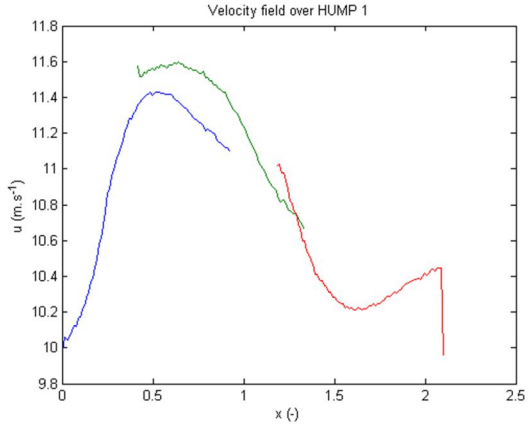

Figure 1. Velocity is increasing above the profile. The height is 25% of channel height.

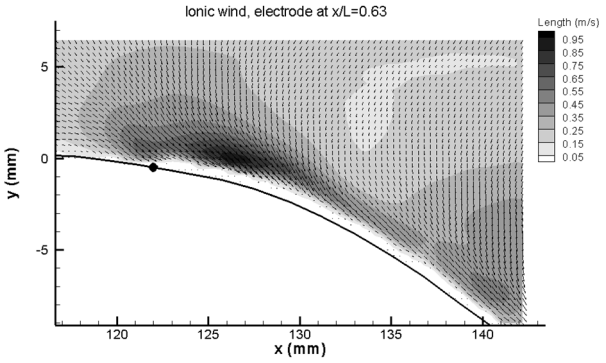

Figure 2. Ionic wind generated in steady air. Wire electrode at x/L = 0.63.

The wake behind the profile is dependent on Reynolds number. The size of the separation bubble is decreasing with increasing channel velocity. The figures 3a,b,c show the flow field made by streamlines visible for the case of no plasma actuation (base case). The flow separates at approx. the distance x/L = 0.64 for all velocities. The recirculation zone is almost negligible for the velocity 20 m·s^{-1} and the identification from PIV acquired data is not easy task. On the other hand, the separation bubble for 5 m·s^{-1} is great and easy to influence. The length of recirculation zone is 130 mm, 92 mm and only 63 mm for the channel velocity 5 m·s^{-1}, 10 m·s^{-1} and 20 m·s^{-1}, respectively. The figure 4 shows the mean velocity vector maps of the wake created by 5 m·s^{-1}.

There can be seen the comparison of the effect of different wire position under 5 m·s^{-1} at the figures 5a, b, c, d. The corresponding positions x/L are 0.63, 0.66, 0.69 and 0.72. From the mean velocity distribution, it can be determined that there is almost no recirculation for the first position for

the steady actuation (5a). The similar situation have been observed during unsteady actuation under 10 Hz and 30%. The actuator placed at the second position can almost fully prevent the creation of the recirculation (there is only small separation bubble up to x/L = 0.77). The situation is completely different when the actuator is further downstream. Since the wire at x/L = 0.69 is behind the natural separation (and the ionic wind origin is even farther), the generated thrust is not able to attached the flow. The energy of the ionic wind is only able to deform the zone of recirculation – separation up to x/L = 1.08 (figure 5c). When the wire is situated at the last position (figure 5d), the effect on the separation bubble size is negligible. However, the topology of the wake structures is changed (e.g. figure 8).

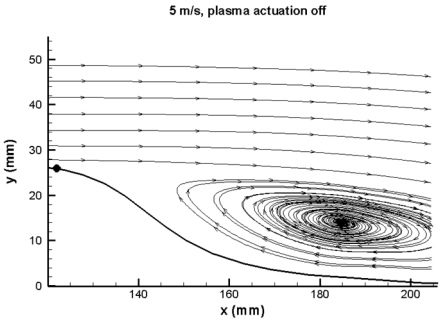

Figure 3a. Wake behind Hump, no actuation, channel velocity 5 m·s^{-1}.

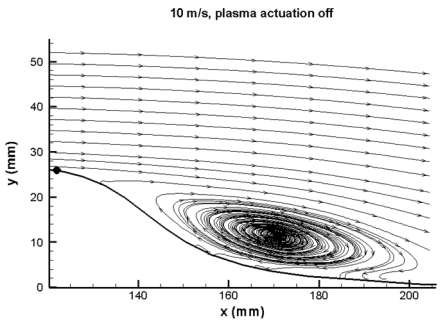

Figure 3b. Wake behind Hump, no actuation, channel velocity 10 m·s^{-1}.

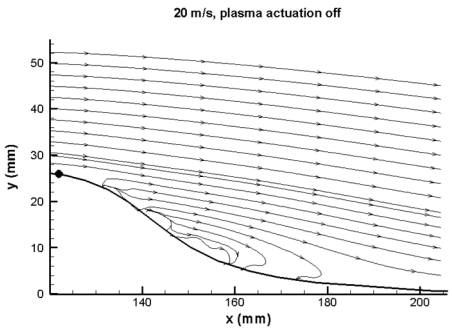

Figure 3c. Wake behind Hump, no actuation, channel velocity 20 m·s^{-1}.

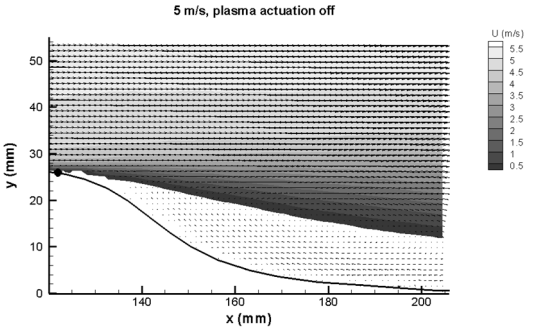

Figure 4. Velocity field, wake behind Hump, no actuation, channel velocity 5 m·s^{-1}.

The influence of the ionic wind becomes less important for the case of higher channel velocities. Only first two position were able to change significantly the wake dimension in the case of 10 m·s^{-1} (reattachement point at x/L = 0.95 or 1.03 instead of 1.12 in base case). The case of the highest velocity seems to be out of the actuator ability. This demonstrated the flow field acquired for the wire in the first two positions. The improvement is present but almost negligible. However, there is significant reduction for the third position. The recirculation zone is already very tiny for base case and it seems that ionic wind occurring in the middle of the bubble can influence the recirculation zone thickness if this zone is not very extensive in normal direction.

The effect on separation point was not observed except the second position. Probably due to suction effect of the actuator, the separation point was shifted about approx. 3 mm downstream.

The effect of the modulation frequency and the duty cycle will be shown in the fourth position of the wire (figures 6a, b and 8). The effect of modulation frequency on separation bubble dimension is tiny. Both the length and the height of the zone are not significantly changed. The effect of duty cycle can be evaluated in dependency of existence of a secondary steady vortex. This steady secondary vortex can be easily evaluated from phase-locked acquired data. This vortex is present in the wake in front of the center of the recirculation and it is cause due to the ionic wind (figure 7). The duty cycle determines the time of plasma actuation and hence the duration time of this secondary vortex during one period. This will appear in mean flow field (figure 6a and 6b).

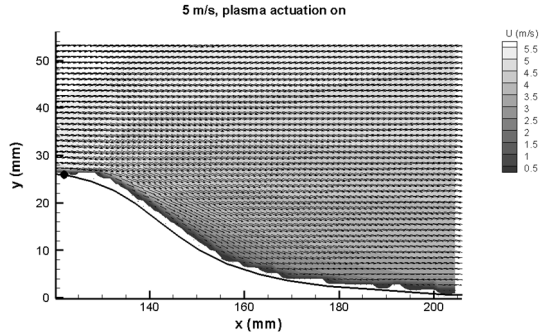

Figure 5a. Effect of ionic wind behind the Hump, channel velocity 5 $m \cdot s^{-1}$, wire electrode at x/L = 0.63.

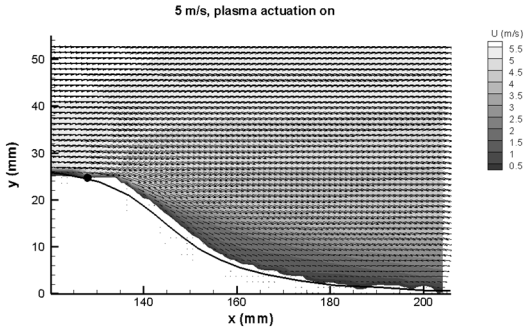

Figure 5b. Effect of ionic wind behind the Hump, channel velocity 5 $m \cdot s^{-1}$, wire electrode at x/L = 0.66.

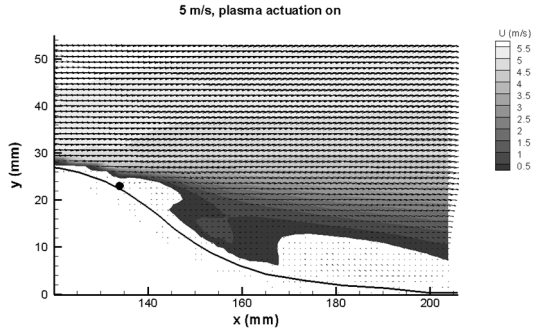

Figure 5c. Effect of ionic wind behind the Hump, channel velocity 5 $m \cdot s^{-1}$, wire electrode at x/L = 0.69.

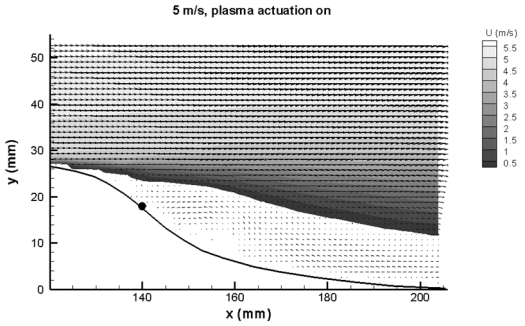

Figure 5d. Effect of ionic wind behind the Hump, channel velocity 5 $m \cdot s^{-1}$, wire electrode at x/L = 0.72.

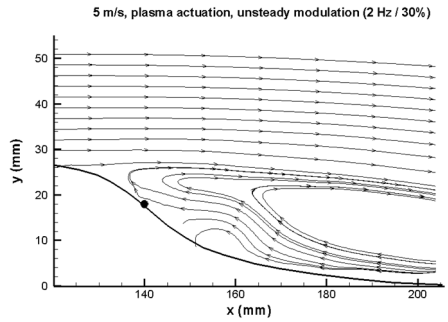

Figure 6a. The effect of duty cycle. Longer time duration of plasma. The secondary vortex is more obvious close to the surface.

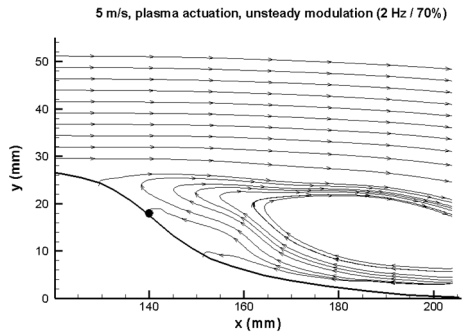

Figure 6b. The effect of duty cycle. Shorter time duration of plasma. The secondary vortex is almost not present close to the surface.

The figure 7 shows the averaging image of the flow field in the seventh phase from twenty. Notice that the secondary structure has opposite sense of rotation. More, this structure is not steady in time, but it is shifting during one period. The convective velocity of the vortex is constant and for the case of 10 Hz and 30% is 0.07 $m \cdot s^{-1}$. Of course, the shape of primary recirculation structure is also changing due to the influence of periodical occurrence of the secondary vortex. This vortex always appears at the beginning of the period.

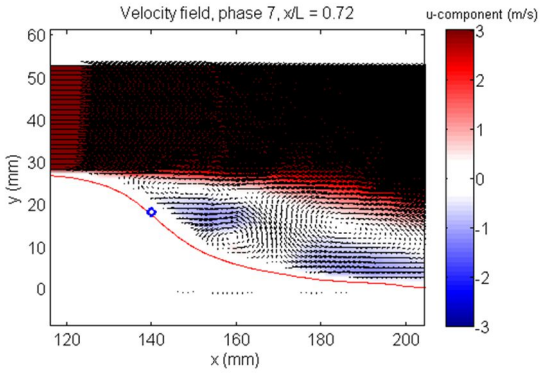

Figure 7. 7th phase of the periodical process – unsteady regime (10 Hz, 30%). The secondary vortex influences the recirculation zone.

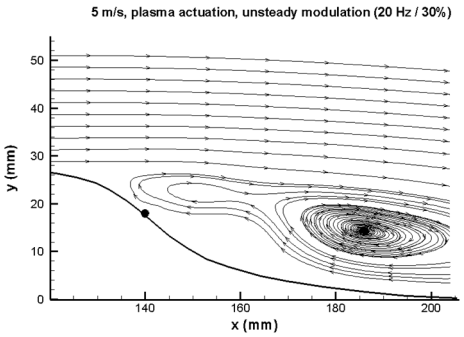

Figure 8. Mean flow field, Unsteady regime (20 Hz, 30%). The secondary vortex influences the recirculation zone.

Stereo PIV measurement in cross-section planes was conducted in order to have the information in the z-coordinates. Since the ionic wind affects the channel flow in parallel sense, there are no important velocity components present in cross-section. This auxiliary measurement has also proved the dimension of the wake under different regimes. The figure 9 reveals the wake under no actuation in x/L = 0.87. POD analysis of this data is considered in the future research.

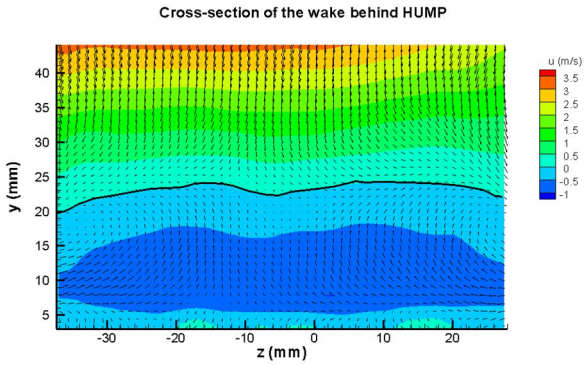

Figure 9. Cross-section plane by stereo PIV measurement at x/L = 0.87. Black solid line denotes the zone of recirculation. 5 $m \cdot s^{-1}$, no actuation.

4. Conclusion

The wake behind the Hump profile (GG body) was experimentally influenced by plasma-induced ionic wind. The plasma actuator was operated in steady as well as in unsteady regime. The unsteady regime was driven by rectangular modulation of voltage waveform. The dimension of the recirculation zone is dependent on Reynolds number.

The wake can be significantly reduced by plasma actuation especially under lower channel velocities**.** There is also an effect for higher velocities. The separation point is not affected but the reattachement point is shifted upstream significantly. Also the topology of the wake can be influence especially when the actuator is placed farther downstream from the natural separation point. The plasma actuation in x/L = 0.66 and especially in x/L = 0.63 has very positive influence and can reduced the wake and the form drag. The effect of modulation frequency seems to be not crucial. However, this should be investigated also for the first two positions more in detail because the effect will differ there more. Duty cycle value will affect the origin and time of duration of the secondary

pseudo-periodical vortical structures. Detailed phase-locked measurements as well as mode analysis have to be done to better investigate this phenomenon.

Especially analysis of dynamics, the measurement with hot wire probes (to determine e.g. frequency spectrum of higher frequencies present in the flow) and energetic balance calculation will be performed in the future. The comparison of the actuator efficiency with other authors will be assigned.

Acknowledgement
The authors gratefully acknowledge financial support of the Grant Agency of the Czech Republic, project No. GP14-25354P.

References

[1] Kurz A et al 2013 *Journal AerospaceLab.* Issue 6 Al06-02
[2] He Ch, Corke T C and Patel M P 2007 *AIAA 45th Aerospace Sciences Meeting*, Paper 2007-0935
[3] Prochazka P and Uruba V 2015 *EPJ Web of Conferences* vol 92 Article number 02074
[4] Prochazka P 2013 Dissertation thesis. Praha ČVUT
[5] Prochazka P and Uruba V 2014 *Journal of Physics: Conf. Ser.*, 530 Article number 012008